Study on the mutual interactions between the parameters of a CANON system and its coping strategy when operating at room temperature (15 to 25 °C) using response surface methodology

Jian Zhou, Guangxu Qin, Jianbing Zhang, Yancheng Li, Qiang He, Yi Han and Benzhou Gong

ABSTRACT

The coping strategy of a CANON (completely autotrophic nitrogen removal over nitrite) reactor working at room temperature was investigated using response surface methodology. The total nitrogen (TN) removal efficiency was taken as a dependent variable. The temperature (X), dissolved oxygen (DO) concentration (Y), and influent nitrogen loading rate (Z) were taken as independent variables. Results showed that the relation of these three independent variables can be described by the TN removal efficiency expressed as $-5.03 + 1.51X + 45.16Y + 30.13Z + 0.26XY + 1.84XZ - 0.04X^2 - 9.06Y^2 - 99.00Z^2$. The analysis of variance proved that the equation is applicable. The response surface demonstrated that the temperature significantly interacts with the DO concentration and influent N loading rate. A coping strategy for the CANON reactor working at room temperature is thus proposed: altering the DO concentration and the N loading rate to counterbalance the impact of low temperature. The verification test proved the strategy is viable. The TN removal efficiency was 91.3% when the reactor was operated under a temperature of 35.0 °C, a DO of 3.0 mg/L, and a N loading rate of 0.70 kgN/(m³ d). When the temperature dropped from 35.0 to 19.2 °C, the TN removal efficiency was kept at 88.7% by regulating the influent N loading rate from 0.7 kgN/(m³ d) to 0.35 kgN/(m³ d) and the DO concentration from 3.0 to 2.6 mg/L.

Key words | autotrophic nitrogen removal, CANON process, room temperature, response surface methodology (RSM), sequencing batch biofilm reactor (SBBR)

Jian Zhou
Guangxu Qin
Jianbing Zhang
Yancheng Li
Qiang He (corresponding author)
Yi Han
Benzhou Gong
Key Laboratory of the Three Gorges Reservoir Region's Eco-environments,
Ministry of Education,
Chongqing University,
174 Shazheng Road,
Chongqing 400045,
China
E-mail: *hq0980@126.com*

INTRODUCTION

Certain kinds of wastewater, such as the leachate of aging landfill, are characterized by low chemical oxygen demand to nitrogen ratios. The conventional way of nitrogen removal through nitrification–denitrification processes is not suitable to apply to these streams. In several systems, autotrophic ammonia removal is observed in streams of high ammonium and low organic carbon loads (Siegrist *et al.* 1998; Keluskar *et al.* 2013). Autotrophic ammonia removal is the combination of the partial nitrification and the anaerobic ammonia oxidation, a process in which the aerobic ammonia-oxidizing bacteria (AAOB) and the anaerobic ammonia-oxidizing bacteria (AnAOB) work together. The nitrite resulting from the partial nitrification process acts as an electron acceptor that helps accomplish the ANAMMOX (anaerobic ammonium oxidation) process. The ANAMMOX process can be described by Equation (1) (Strous *et al.* 1999):

$$NH_4^+ + 1.3NO_2^- + 0.066HCO_3^- + 0.13H^+ \rightarrow 1.02N_2 + 0.26NO_3^- + 0.066CH_2O_{0.5}N_{0.15} + 2H_2O \quad (1)$$

Many processes are involved in producing a better synergistic effect between AAOBs and AnAOBs. AAOBs and AnAOBs can work in separate units (Sharon-ANAMMOX) or together in one oxygen-limited tank (CANON – completely autotrophic nitrogen removal over nitrite) (van Dongen *et al.* 2001; Sliekers *et al.* 2003). For the latter system, a biofilm reactor is applied. The partial nitrification process and the ANAMMOX processes can occur in the

doi: 10.2166/wst.2014.062

same piece of biofilm. AAOBs are located on the outer side of the biofilm, where they oxidize ammonia into nitrite. The inner side of the biofilm constitutes an absolutely anaerobic space, which can be an appropriate shelter for the AnAOBs.

Temperature is a governing factor of the CANON process. The partial nitrification process encounters problems under a low temperature, because nitrite-oxidizing bacteria, a competitor of AAOB, prosper under the same condition (Hellinga *et al.* 1998; van Hulle *et al.* 2007). Any further decrease in the temperature reduces the activity of both AAOBs and AnAOBs. Although few CANON reactors have succeeded in working under a comparatively low temperature (Liu *et al.* 2012; Daverey *et al.* 2013), most researchers ensure that their CANON reactors work in a temperature range between 30 and 35 °C (Third *et al.* 2001; Park *et al.* 2010; Zhang *et al.* 2010). Recently, a few reports have been published on the strategy for the system to cope with a low temperature. If the CANON process can be widely made to operate at a lower temperature, its application potential can be extended (Jetten *et al.* 1997).

AAOBs can accomplish partial nitrification from 4 to 45 °C (Vazquez-Padin *et al.* 2009), whereas AnAOBs can sustain their activity in a temperature range from 6 to 43 °C (Jetten *et al.* 1999; Dalsgaard & Thamdrup 2002). The two kinds of bacteria share a wide temperature application range. And once they cooperate well under a comparatively low temperature (6 to 25 °C), the operation of the CANON system can be stabilized at that condition. Although a low temperature reduces the activity of both bacteria, some strategies can help the system to work with a relatively high efficiency.

The response surface methodology (RSM) is a collection of mathematical and statistical techniques. A certain experiment is conducted to fit a response surface, which can simulate the real surface in the ultimate state. It can be used to optimize processes and analyze the interactions between the affecting factors (Montgomery 2001; Myers & Montgomery 2001). The method is characterized by few experiment times and high accuracy. It has been adopted in research in environmental science, such as the optimization of ammonia nitrogen removal from landfill leachate (Bashir *et al.* 2010), and the optimization of the coagulation/flocculation process (Khayet *et al.* 2011).

This study attempts to formulate a strategy that can assist the CANON reactor to work at room temperature, and thereby expand the engineering application of the process. The Box–Behnken design (BBD) (Draper *et al.* 1994; Montgomery 2001) and RSM have been applied to achieve this task. The mutual interactions between the parameters of the CANON reactor are analyzed to derive an appropriate strategy. Then, an experiment is performed to inspect and verify the analysis above.

METHODS

Reactor description

As shown in Figure 1, the experiment was conducted in a sequencing batch biofilm reactor (SBBR) with a working volume of 12 L. The unit had the following dimensions: a height of 500 mm and an inner diameter of 200 mm, with the height to the diameter ratio being 2.5. Air was supplied to the bottom of the reactor by using an air pump to promote the transfer of oxygen into the bulk liquid. A rotameter was also placed between the air pump and the tank to regulate the dissolved oxygen (DO) concentration in the bulk. A semi-soft filler was used as the biomass carrier and the packing rate was 50% (V/V).

Operational strategy

Six previously developed CANON reactors were selected for the RSM experiment and the verification test. For feeding with a high concentration (NH_4^+-N: 2,000 mg/L) stream, biofilm thickness of these reactors exceed 8,000 μm. The DO concentration of the bulk was higher than that close to the biofilm in these reactors. All the reactors were kept running for more than 1 year, and were placed under a similar condition before the beginning of each experiment.

An artificial wastewater was used to facilitate the BBD. The right amount of NH_4-HCO_3 was added into tap water, making the NH_4^+-N concentration of the solution to be 2,000 mg/L. The composition of the synthetic media in mg/L was as follows: KH_2PO_4: 25; EDTA: 25; $FeSO_4$: 6.25; $MgSO_4 \cdot 7H_2O$: 200; $CaCl_2$: 300; trace solution: 1.25 and the right amount of $NaHCO_3$ to regulate pH to 8.0.

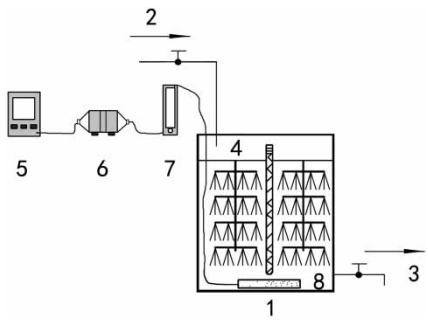

Figure 1 | The reactor (1 – SBBR reactor, 2 – influent inlet, 3 – effluent outlet, 4 – biomass carrier, 5 – time controller, 6 – air pump, 7 – rotameter, 8 – aeration device).

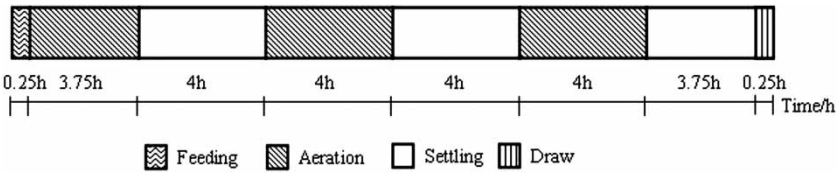

Figure 2 | Distribution of the operational cycles.

The reactors had no carbon supply. The N loading rate was controlled by the drain ratio. When the drain ratios were 0.20, 0.35, and 0.50, the N loading rates were 0.4, 0.7, and 1.0 kgN/(m^3 d) respectively. The SBBR were operated in cycles of 24 h distributed according to the scheme described in Figure 2. Nitrogen species were tested and analyzed according to the standard methods of the American Public Health Association (APHA 2005); temperature and DO concentration were tested by a Hach portable DO meter.

The experiment was undertaken in two stages. Part 1 consisted of the experiment for the RSM analysis. In this stage of the experiment, the reactor was placed in a thermostatic chamber, for the control of the temperature. All of the reactors remained stable for more than 2 months at this stage; then average total nitrogen (TN) removal efficiency was determined to support the RSM analysis. Part 2 consisted of the verification test, which was conducted in the local autumn. For the first 2 weeks of this stage, the reactor was in a thermostatic chamber. Then the reactor was placed in an ambient temperature with no temperature control.

The RSM design

Three steps are involved, including the statistical design of the experiments, the obtaining of the equation, and the applicability examination (Montgomery 2001; Bas & Boyaci 2007). The experimental design was based on BBD; TN removal efficiency, the governing evaluation factor of the performance of the CANON reactor, was selected as the dependent variable in the experiment. A total of three independent variables were used: the temperature of the reactor, the DO concentration during aeration, and the influent N loading rate.

Each of the independent variables had three levels. Table 1 shows the levels and their corresponding actual values. The chosen independent variables used in this experiment were coded according to Equation (2):

$$x_i = (X_i - X_0)/\Delta x \tag{2}$$

Table 1 | Levels and actual values of each variable

Range and level	Parameter A temperature (°)	Parameter B DO concentration (mg/L)	Parameter C N loading rate (kgN/(m^3 d))
+1	35	4.0	1.0
0	22	2.5	0.7
−1	9	1.0	0.4

where x_i is the coded value of the ith variable; X_i represents the uncoded value of the ith test variable; X_0 is the uncoded value of the ith test variable at the center point.

The selection of the model depends on the experiment result (Montgomery 2001; Myers & Montgomery 2001). Following the BBD, a total of 17 experiments were conducted. The experimental scheme and result are both listed in Table 2. The central point has five repetitive experiments to improve the precision. Based on the results, a second-order polynomial model was better suited to describe the correlation between the input variables and their output response (Myers *et al.* 2009). Equation (3) shows the empirical second-order polynomial model:

$$y = \beta_0 + \sum_{i=1}^{k} \beta_i x_i + \sum_{i=1}^{k} \beta_{ii} x_i^2 + \sum_{i} \sum_{j} \beta_{ij} x_i x_j + \varepsilon \tag{3}$$

where y is the predicted TN removal efficiency response; x_i represents the coded variables; β_0, β_i, β_{ii}, β_{ij} are the regression coefficients and ε is the stochastic term, which is supposed to have Gaussian distribution.

RESULTS AND DISCUSSION

Proof of model

The following coded equation (Equation (4)) for the TN removal efficiency was developed from Equation (3); the coefficients are listed in Table 3, which were fixed by multiple regression analysis based on the experimental data.

Table 2 | Box–Behnken design and results

				Factors			
Run	A	B	C	Temperature (°)	DO concentration (mg/L)	N loading rate (kgN/(m^3 d))	TN removal efficiency (%)
1	0	0	0	22	2.5	0.7	78.5
2	0	1	−1	22	4.0	0.4	78.9
3	1	−1	0	35	1.0	0.7	51.6
4	−1	−1	0	9	1.0	0.7	27.2
5	1	1	0	35	4.0	0.7	84.2
6	0	−1	1	22	1.0	1.0	18.6
7	1	0	1	35	2.5	1.0	74.5
8	0	0	0	22	2.5	0.7	78.4
9	0	0	0	22	2.5	0.7	78.4
10	0	0	0	22	2.5	0.7	78.3
11	−1	0	−1	9	2.5	0.4	63.9
12	−1	1	0	9	4.0	0.7	39.2
13	1	0	−1	35	2.5	0.4	93.2
14	0	1	1	22	4.0	1.0	31.1
15	−1	0	1	9	2.5	1.0	16.5
16	0	0	0	22	2.5	0.7	78.3
17	0	−1	−1	22	1.0	0.4	67.9

Table 3 | Significance of regression coefficients

Model term	Estimated coefficients (coded)	*P*-value with BC	*P*-value without BC
Constant	78.42	<0.0001	<0.0001
A	19.59	<0.0001	<0.0001
B	8.51	0.034	0.017
C	−20.40	<0.0001	<0.0001
AB	5.15	0.1065	0.0834
AC	7.18	0.0365	0.0249
BC	0.38	0.8965	–
A^2	−7.49	0.0280	0.0185
B^2	−20.39	0.0001	<0.0001
C^2	−8.91	0.0134	0.0080

The *P*-value of the BC term was more than 0.1, and thus was removed from the equation. And as Table 3 shows, *P*-values of other terms were all less than 0.1, indicating they all have significant influence on the regression equation:

$$\text{TN removal efficiency} = 78.42 + 19.59A + 8.51B - 20.40C + 5.15AB + 7.18AC - 7.49A^2 - 20.39B^2 - 8.91C^2 \quad (4)$$

The results of the analysis of variance (ANOVA) for Equation (4) are presented in Table 4. The *P*-value (Prob > *F*) of the model was relatively low ($P < 0.0001$), indicating that the model is significant. The other indices must be in accordance with *F* (lack of fit) > 0.1, $R^2 > 0.95$, (Adj R^2 – Pre R^2) < 0.2, C.V. < 10%, Pre $R^2 > 0.7$, Adeq Precision > 4.011 (Myers & Montgomery 2001; Arslan-Alaton *et al.* 2009). Table 4 shows the index of Equation (4) that could satisfy the requirements. *P*-values of linear, square, and interaction were all less than 0.05, indicating these terms are all significant. Therefore, ANOVA shows that Equation (4) is appropriate in describing the relation between the parameters (temperature, DO concentration of the bulk, and N loading rate) and the response variable (TN removal efficiency). Transforming the coded value to actual value resulted in Equation (5), which could describe the actual relation:

$$\text{TN removal efficiency} = -5.03 + 1.51X + 45.16Y + 30.13Z + 0.26XY + 1.84XZ - 0.04X^2 - 9.06Y^2 - 99.00Z^2 \quad (5)$$

where X is the temperature; Y is the DO concentration; Z is the N loading rate.

Table 4 | Analysis of variance

Source	Sum of squares	Df	Mean square	*F*-value	*P*-value Prob > *F*
Model	9812.50	8	1226.56	45.19	<0.0001
Linear	6978.34	3	2326.11	85.71	<0.0001
Square	2319.85	3	773.28	28.49	0.0001
Interaction	312.01	2	156.01	5.74	0.0284
Residual	217.14	8	27.14		
Lack of fit	216.39	4	54.10	238.29	<0.0001
Pure error	0.75	4	0.19		
Total	10,029.64	16			
Std Dev. = 5.21	$R^2 = 0.9784$	Adj. $R^2 = 0.9567$			
Pre. $R^2 = 0.7605$	C.V. = 8.53%	Adeq. precision = 21.298			

Std Dev.: standard deviation; Pre.: predicted; Adj.: adjusted; C.V.: coefficient of variation; Adeq.: adequate.

Analysis of the response surface

Three-dimensional plots could be generated to visualize the response surfaces. The cumulative effects of any two variables of the experiment could be displayed while keeping the other factor constant. The results are listed in Figures 3–5.

In these figures, the shape of the contour line describes the interaction effect between the parameters. An elliptical contour line indicates that the two factors interact significantly, whereas a circle shows the two factors interact indistinctly. Thus, Figure 3(b) illustrates that temperature and DO concentration interact significantly, which means that the dropping of temperature negatively impacts the system and DO concentration can be regulated to counterbalance this impact.

Under a constant N loading rate of 0.7 kgN/(m³ d) as shown in Figure 3(a), and when the temperature was dropped from 35 to 22 °C, the TN removal efficiency also dropped accordingly. However, the TN removal efficiency was 80%, a relatively high value, when the two parameters were as follows: a temperature of 22 °C and a DO concentration of 2.7 mg/L. When the temperature and DO concentration were set at 22 °C and 1.0 mg/L, respectively, the removal efficiency dropped sharply to 50%. When the influent loading rate was set to 0.4 kgN/(m³ d) or 1.0 kgN/(m³ d), a similar result was observed.

In Figure 4(b), the contour line tends to be straight, which indicates that the temperature and the influent N loading rate interact extremely significantly. As analyzed before, when a drop in the temperature negatively impacts the system, the influent N loading rate can be restricted to

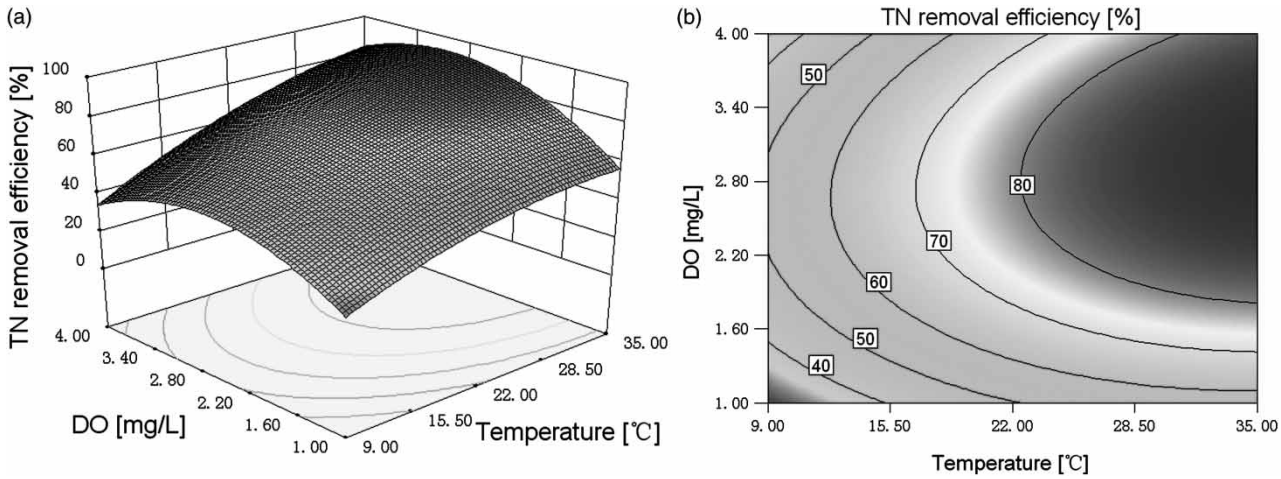

Figure 3 | Response surface graphs when the influent N loading rate is 0.7 kgN/(m³ d). (a) 3D surface, (b) contour.

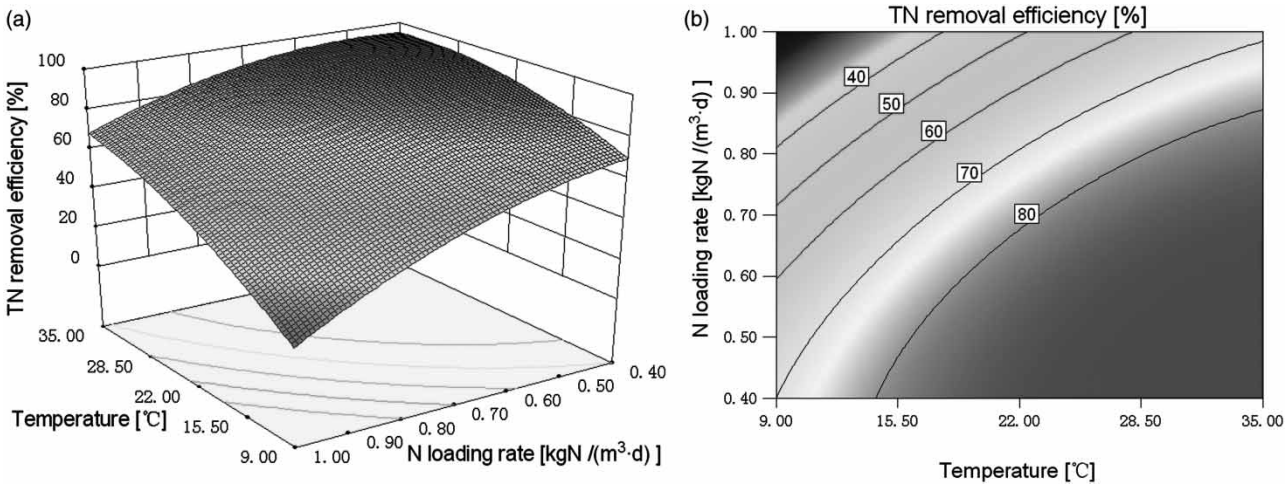

Figure 4 | Response surface graphs when the DO concentration is 2.5 mg/L. (a) 3D surface, (b) contour.

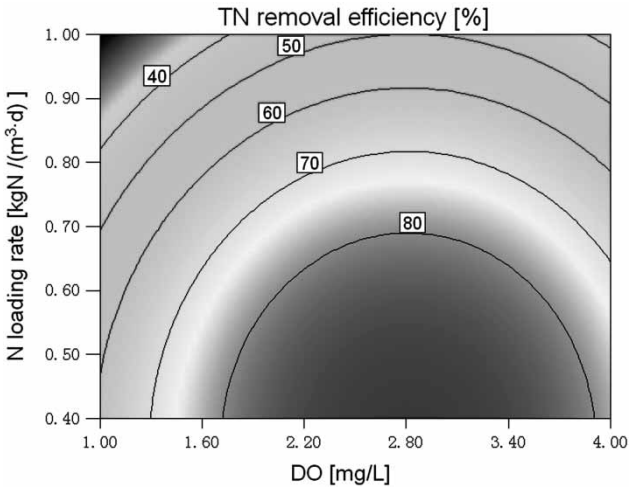

Figure 5 | Response surface graph (counter) when the temperature is 22 °C.

counterbalance that impact as well. Furthermore, because of the extremely significant interaction of the two factors, the counterbalance effect this time is greater than that of the DO concentration.

Under a DO concentration of 2.5 mg/L, and when the temperature is decreased from 35 to 15 °C, the TN removal efficiency also decreased sharply. However, a relatively high TN removal efficiency of about 80% could be obtained if the influent N loading rate was set to 0.4 kgN/(m³ d). Furthermore, if the N loading rate was set to 1.0 kgN/(m³ d), the removal percentage would be 33%. When the DO concentration was fixed at 1.0 or 4.0 mg/L, similar results were observed.

Unlike the figures above, the contour line tends to be circular in Figure 5, which indicates that no significant interaction occurs between DO concentration and influent N loading rate. Thus, their variation could counterbalance the impact of temperature separately and independently. As such, when the CANON reactor enters the condition of low temperature, the coping strategy can be as follows: controlling and regulating the parameters of influent N loading rate and DO concentration, via the counterbalance effect, to keep a relatively high efficiency. Specifically, when temperature dropped, N loading rate should be reduced and DO should be regulated to a proper value based on Equation (5) to maintain a comparatively high efficiency. For example, when temperature, DO and N loading rate are 35 °C, 3.0 mg/L and 0.7 kgN/(m³ d), the estimated TN removal efficiency is 92.8%; if temperature drops to 15 °C, DO and N loading rate can be regulated to 2.4 mg/L and 0.25 kgN/(m³ d), to get an expected TN removal of 81.6%.

Verification test

As shown in Figure 6, during the first 2 weeks the reactor ran under a temperature of 35.0 °C. The N loading rate and the DO concentration were 0.7 kgN/(m³ d) and 3.0 mg/L, respectively. The reactor achieved an average TN removal efficiency of 91.3%. On the 14th day, the reactor began to have an ambient temperature. Afterward, the average temperature of the reactor was 19.2 °C. Based on the strategy and Equation (5), influent N loading rate was regulated to 0.35 kgN/(m³ d) and DO concentration to 2.6 mg/L.

After debugging, the CANON reactor showed an improved performance on the 33rd day. Afterward, the running status of the reactor stabilized, with an average TN

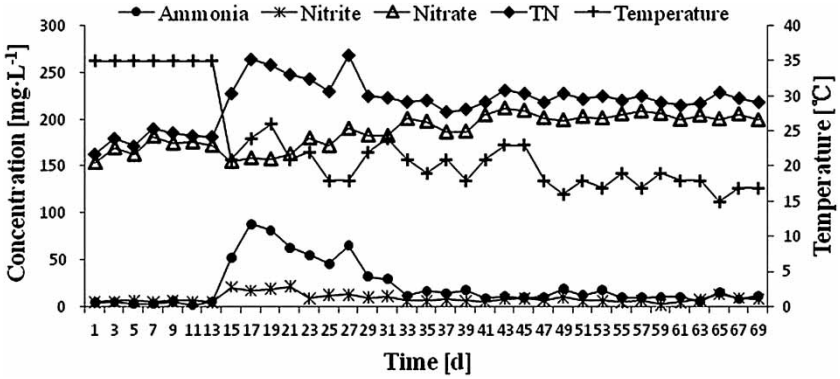

Figure 6 | Results of the verification test.

removal efficiency of 88.7%. The strategy was proved to be viable. Nitrate did not accumulate, with a concentration between 187.8 and 220.9 mg/L. The NOBs remained inhabited. The average effluent ammonia and effluent nitrite were 12.0 and 6.3 mg/L, respectively. The AAOB and the AnAOB cooperated well (Strous *et al*. 1999), indicating that the drop in temperature merely brought down the activity of the two bacteria separately. However, the synergy between them could be maintained by regulating the other parameter.

CONCLUSION

BBD and response surface were involved in the study of the interaction between DO concentration, N loading rate, and temperature in the CANON reactor. The temperature showed a significant interaction with the N loading rate and the DO concentration. A strategy to cope with the room temperature for the CANON system was proposed: altering the parameters of N loading rate and DO concentration to counterbalance the impact of low temperature. The verification test proved the viability of the strategy, and indicated that, with its adoption, the CANON reactor could be made to run with a relatively high efficiency under room temperature.

ACKNOWLEDGEMENT

The authors wish to acknowledge the Major Science and Technology Program for Water Pollution Control and Treatment of China (2012ZX07307-002) for the financial support of this study.

REFERENCES

APHA 2005 *Standard Methods for the Examination of Water and Wastewater* 21st edn, American Public Health Association/American Water Works Association/Water Environment Federation, Washington, DC, USA.

Arslan-Alaton, I., Tureli, G. & Olmez-Hanci, T. 2009 Treatment of azo dye production wastewaters using Photo-Fenton-like advanced oxidation processes: optimization by response surface methodology. *Journal of Photochemistry and Photobiology A-Chemistry* **202** (2–3), 142–153.

Bas, D. & Boyaci, I. H. 2007 Modeling and optimization I: usability of response surface methodology. *Journal of Food Engineering* **78** (3), 836–845.

Bashir, M., Aziz, H., Yusoff, M. & Adlan, M. 2010 Application of response surface methodology (RSM) for optimization of ammoniacal nitrogen removal from semi-aerobic landfill leachate using ion exchange resin. *Desalination* **254** (1–3), 154–161.

Dalsgaard, T. & Thamdrup, B. 2002 Factors controlling anaerobic ammonium oxidation with nitrite in marine sediments. *Applied and Environmental Microbiology* **68** (8), 3802–3808.

Daverey, A., Su, S. H., Huang, Y. T., Chen, S. S., Sung, S. W. & Lin, J. G. 2013 Partial nitrification and anammox process: a method for high strength optoelectronic industrial wastewater treatment. *Water Research* **47** (9), 2929–2937.

Draper, N. R., Pozueta, L., Davis, T. P. & Grove, D. M. 1994 Isolation of degrees of freedom for Box-Behnken Designs. *Technometrics* **36** (3), 283–291.

Hellinga, C., Schellen, A., Mulder, J. W., van Loosdrecht, M. & Heijnen, J. J. 1998 The SHARON process: an innovative method for nitrogen removal from ammonium-rich waste water. *Water Science and Technology* **37** (9), 135–142.

Jetten, M., Horn, S. J. & van Loosdrecht, M. C. M. 1997 Towards a more sustainable municipal wastewater treatment system. *Water Science and Technology* **35** (9), 171–180.

Jetten, M., Strous, M., van de Pas-Schoonen, K. T., Schalk, J., van Dongen, U., van de Graaf, A. A., Logemann, S., Muyzer, G., van Loosdrecht, M. & Kuenen, J. G. 1999 The anaerobic

oxidation of ammonium. *FEMS Microbiology Reviews* **22** (5), 421–437.

Keluskar, R., Nerurkar, A. & Desai, A. 2013 Development of a simultaneous partial nitrification, anaerobic ammonia oxidation and denitrification (SNAD) bench scale process for removal of ammonia from effluent of a fertilizer industry. *Bioresource Technology* **130**, 390–397.

Khayet, M., Zahrim, A. Y. & Hilal, N. 2011 Modelling and optimization of coagulation of highly concentrated industrial grade leather dye by response surface methodology. *Chemical Engineering Journal* **167** (1), 77–83.

Liu, T., Li, D., Zeng, H. P., Li, X. K., Liang, Y. H., Chang, X. Y. & Zhang, J. 2012 Distribution and genetic diversity of functional microorganisms in different CANON reactors. *Bioresource Technology* **123**, 574–580.

Montgomery, D. C. 2001 *Design and Analysis of Experiments*. 5th edn, Wiley, New York.

Myers, R. H. & Montgomery, D. C. 2001 *Response Surface Methodology*. 2nd edn, Wiley, New York.

Myers, R. H., Montgomery, D. C. & Anderson-Cook, C. M. 2009 *Response Surface Methodology: Process and Product Optimization Using Designed Experiments*. 3rd edn, Wiley, New Jersey.

Park, H., Rosenthal, A., Jezek, R., Ramalingam, K., Fillos, J. & Chandran, K. 2010 Impact of inocula and growth mode on the molecular microbial ecology of anaerobic ammonia oxidation (anammox) bioreactor communities. *Water Research* **44** (17), 5005–5013.

Siegrist, H., Reithaar, S. & Lais, P. 1998 Nitrogen loss in a nitrifying rotating contactor treating ammonium rich leachate without organic carbon. *Water Science and Technology* **37** (4–5), 589–591.

Sliekers, A. O., Third, K. A., Abma, W., Kuenen, J. G. & Jetten, M. 2003 CANON and Anammox in a gas-lift reactor. *FEMS Microbiology Letters* **218** (2), 339–344.

Strous, M., Kuenen, J. G. & Jetten, M. 1999 Key physiology of anaerobic ammonium oxidation. *Applied and Environmental Microbiology* **65** (7), 3248–3250.

Third, K. A., Sliekers, A. O., Kuenen, J. G. & Jetten, M. 2001 The CANON system (Completely Autotrophic Nitrogen-removal Over Nitrite) under ammonium limitation: interaction and competition between three groups of bacteria. *Systematic and Applied Microbiology* **24** (4), 588–596.

van Dongen, U., Jetten, M. & van Loosdrecht, M. 2001 The SHARON-Anammox process for treatment of ammonium rich wastewater. *Water Science and Technology* **44** (1), 153–160.

van Hulle, S. W. H., Volcke, E. I. P., López Teruel, J., Donckels, B. & van Loosdrecht, M. 2007 Influence of temperature and pH on the kinetics of the SHARON nitritation process. *Journal of Chemical Technology and Biotechnology* **82** (5), 471–480.

Vazquez-Padin, J. R., Figueroa, M., Fernandez, I., Mosquera-Corral, A., Campos, J. L. & Mendez, R. 2009 Post-treatment of effluents from anaerobic digesters by the Anammox process. *Water Science and Technology* **60** (5), 1135–1143.

Zhang, Z. J., Chen, S. H., Wu, P., Lin, L. F. & Luo, H. Y. 2010 Start-up of the Canon process from activated sludge under salt stress in a sequencing batch biofilm reactor (SBBR). *Bioresource Technology* **101** (16), 6309–6314.

First received 20 November 2013; accepted in revised form 23 January 2014. Available online 7 February 2014